

# Elucidating the Anti-Metastatic Potency of *Morinda citrifolia* L. Compounds via Targeting MMP9: An Integrative Network Pharmacology and Molecular Dynamics Simulation

Wira Eka Putra<sup>1,\*,#</sup> , Arief Hidayatullah<sup>2,#</sup> , Diana Widiastuti<sup>3</sup> , Hary Isnanto<sup>4</sup> , Muhammad Fikri Heikal<sup>5</sup>  and Sustiprijatno Sustiprijatno<sup>6</sup> 

<sup>1</sup>Biotechnology Study Program, Department of Applied Sciences, Faculty of Mathematics and Natural Sciences, Universitas Negeri Malang, East Java, Indonesia.

<sup>2</sup>Democratic Governance and Poverty Reduction Unit, United Nations Development Programme, Eijkman-RSCM Building, Jakarta, Indonesia.

<sup>3</sup>Department of Chemistry, Faculty of Mathematics and Natural Science, Universitas Pakuan, West Java, Indonesia.

<sup>4</sup>Department of Biochemical Technology, School of Bioresources and Technology, King Mongkut's University of Technology Thonburi, Bangkok, Thailand.

<sup>5</sup>Tropical Medicine Graduate Program, Faculty of Medicine, Khon Kaen University, Khon Kaen, Thailand.

<sup>6</sup>Research Center for Applied Botany, National Research and Innovation Agency, West Java, Indonesia.

## ABSTRACT

Metastasis is a major cause of mortality in breast cancer, making it a critical target in therapeutic strategies. *Morinda citrifolia* L., a tropical medicinal plant, has shown promise due to its bioactive compounds. This study investigates the anti-metastatic potential of *M. citrifolia* compounds by targeting matrix metalloproteinase-9 (MMP-9), a key protein involved in tumor invasion and metastasis. An integrative *in silico* approach was employed, including drug-likeness and toxicity screening, biological activity prediction, membrane permeability analysis, target protein identification, enrichment analysis, protein structure validation, molecular docking, and molecular dynamics simulations. Among the screened compounds, quercetin and obtusin exhibited strong binding affinity for MMP-9. We suggest that quercetin inhibits MMP-9 via zinc chelation and multi-point hydrogen bonding, while obtusin acts through cavity remodeling and potential allosteric modulation. Both compounds overlap with Marimastat's binding site, an established MMP-9 inhibitor, but engage the enzyme through distinct molecular interactions, highlighting their complementary mechanisms. Quercetin and obtusin from *M. citrifolia* inhibit MMP-9 through different yet complementary modes of action, suggesting their potential as anti-metastatic agents. These findings support further investigation through *in vitro* and *in vivo* studies to validate their therapeutic efficacy.

## KEYWORDS

*In silico*, metastasis, MMP9, natural products, noni fruit

Received 12 July 2025, revised 4 October 2025, accepted 30 October 2025

## INTRODUCTION

Breast cancer is still considered the most commonly diagnosed cancer among women globally, and it continues to be a leading cause of cancer-related deaths.<sup>1</sup> In 2020, an estimated 2.3 million new cancer cases were reported, accounting for one in four newly diagnosed cases, along with 685,000 cancer-related deaths, representing 1 in 6 total deaths.<sup>2</sup> By 2030, it is projected that the global incidence of newly diagnosed breast cancer cases will rise to 2.7 million annually, with approximately 870,000 deaths each year. The risk of developing breast cancer is influenced by a range of factors, including genetic mutations, ethnicity, lifestyle choices such as physical activity, obesity, alcohol consumption, smoking, and exposure to environmental chemicals, and other contributing factors.<sup>3</sup>

To a great extent, the high incidence and mortality rates of breast cancer are primarily attributed to the development of metastasis, which is a complex process in which a primary tumor gives rise to a distant secondary tumor. The diagnosis of metastatic cancer is typically regarded as the final stage for most cancer types.<sup>4</sup> Advanced-stage breast cancer, often characterized by metastasis, is generally associated with a poor prognosis.<sup>5</sup> While early detection of breast cancer before metastasis significantly improves survival rates, it is often diagnosed, primarily after metastasis has already taken place.<sup>4</sup>

Metastasis is a highly complex process involving various cellular mechanisms. It is influenced not only by genetic changes within cancer cells but also by the tumor's surrounding microenvironment,

including the role of tumor-associated macrophages, which contribute to breast cancer metastasis.<sup>6</sup> Among molecules implicated in metastasis, the matrix metalloproteinase-9 (MMP-9) has emerged as a key mediator.<sup>7,8</sup> This protein is involved in multiple signaling pathways that promote cancer progression.<sup>9</sup> In breast cancer, MMP-9 expression is upregulated by co-stimulation with TNF- $\alpha$  and TGF- $\beta$ <sup>10</sup>. Furthermore, MMP-9 degrades the extracellular matrix, facilitating the detachment and migration of tumor cells.<sup>11</sup> Consequently, targeting MMP-9 with therapeutic agents holds significant potential as an anti-metastatic strategy in breast cancer treatment.

In recent years, several synthetic MMP-9 inhibitors have been computationally designed.<sup>12</sup> Some of these compounds have advanced to preliminary *in vitro* testing using various cancer cell lines. Notably, certain inhibitors have demonstrated high selectivity for MMP-9 over other members of the MMP family, which is essential to reduce off-target effects and toxicity. For instance, three aryl-amide derivatives have shown significant inhibitory activity against the 4T1 breast cancer cell line.<sup>13</sup> *In silico* molecular docking studies further support the therapeutic potential of these compounds, revealing strong binding affinities at the MMP-9 active site.<sup>14</sup> Despite these promising preclinical findings, none of these synthetic inhibitors have yet received FDA approval for clinical use.<sup>12</sup>

In addition to synthetic inhibitors, several bioinformatics-based screenings have been conducted to identify potential MMP-9 inhibitors derived from natural products. Previous studies have reported that certain natural compounds from *Juniperus communis* and *Hibiscus esculentus* exhibit strong inhibitory effects against MMP-9.<sup>15,16</sup> Furthermore, flavonoid compounds have demonstrated significant activity by effectively binding to the active site of the

\*To whom correspondence should be addressed  
Email: wira.putra.fmipa@um.ac.id

#These authors contributed equally to this work

enzyme.<sup>17</sup> Another compelling example is a cinnamic acid derivative that has demonstrated strong MMP-9 inhibition. This natural compound not only exhibit high binding affinity but also display considerable stability, highlighting their potential as drug candidates for the treatment of various diseases.<sup>18</sup> Given the promising bioactivity of natural-derived products, further exploration and screening of additional natural compounds are strongly warranted.

Natural products offer significant advantages compared to synthetic compounds, including vast scaffold diversity and structural complexity, making them promising drug candidates.<sup>19</sup> *M. citrifolia* L., commonly known as noni fruit, is widely found in Southeastern Asia. A previous study demonstrated that this plant possesses multiple pharmacological activities, including anticancer effects.<sup>20,21</sup> One of the key factors contributing to its therapeutic effects is the presence of major bioactive compounds such as 4-hydroxycoumarin, caffeic acid, chlorogenic acid, coumalic acid, ferulic acid, isoquercetin, kaempferol-3-rutinoside, obtusin, p-hydroxybenzoic acid, quercetin, and rutinum.<sup>22</sup>

Although numerous studies have reported the anticancer properties of *M. citrifolia* L.,<sup>20,21,23</sup> limited research has specifically addressed the inhibitory effects of its bioactive compounds on cancer metastasis. Hence, the purpose of this study is to investigate the potential of the major bioactive compounds of *M. citrifolia* L. as anti-cancer drug candidates, with a particular focus on their role in inhibiting metastasis. To do this, the plan is to identify and evaluate the major bioactive compounds of *M. citrifolia* L. reported in phytochemical studies and, to assess the interaction of these compounds with MMP9, a key protein associated with cancer metastasis. An integrative *in silico* analysis to evaluate the anti-metastatic activity of *M. citrifolia* major bioactive compounds targeting MMP9 will be done. This strategy, includes molecular docking, pharmacokinetics, and network-based analyses.

## EXPERIMENTAL

This study employed *in silico* approaches, including drug-likeness and toxicity screening, activity and permeability prediction, target identification, enrichment analysis, structure validation, and molecular docking with dynamics simulation. The workflow is shown in Figure 1.

### Drug-likeness screening and toxicity prediction

Virtual screening was conducted on the major active compounds of *M. citrifolia*, which include 4-hydroxycoumarin, caffeic acid, chlorogenic acid, coumalic acid, ferulic acid, isoquercetin, kaempferol-3-rutinoside, obtusin, p-hydroxybenzoic acid, quercetin, and rutinum.<sup>22</sup> The drug-likeness screening was performed based on several parameters, including the Lipinski, Ghose, Veber, Egan, and Muegge rules. The SwissADME webserver (<http://www.swissadme.ch/>) was used to evaluate the drug-likeness properties.<sup>24</sup> Compounds that met the drug-likeness criteria were further subjected to toxicity evaluations, which included toxicity class prediction, lethal dose 50% (LD50) prediction, and the assessment of potential toxicity effects on organs such as the liver (hepatotoxicity), brain (neurotoxicity), heart (cardiotoxicity), as well as carcinogenicity, immunotoxicity, and cytotoxicity. Toxicity predictions were made using the ProTox 3.0 webserver (<https://tox.charite.de/prottox3/>).<sup>25</sup>

### Biological activity and membrane permeability prediction

Biological activity prediction was conducted on the hit-to-lead compounds that successfully passed the drug-likeness screening and toxicity evaluation. The biological activities of these compounds were predicted using the Way2Drug (<https://www.way2drug.com/passonline/>) webserver.<sup>26</sup> Additionally, the membrane permeability of these compounds, a critical property for drug candidates, was explored using the PerMM server and database (<https://permm.phar.umich.edu/>).<sup>27</sup> The predictions were performed under experimental conditions that simulated physiological parameters, with a temperature of 310 Kelvin and a pH of 7.4.

### Target protein determination

Each compound possesses unique characteristics defined by its chemical properties, which influence its interaction with protein targets associated with diseases, including cancer. In this study, target protein prediction was performed on the hit-to-lead compounds to identify their specific target proteins using the SwissTargetPrediction webserver (<http://www.swisstargetprediction.ch/>).<sup>28</sup> Furthermore, a Venn diagram tool (<http://bioinformatics.psb.ugent.be/webtools/Venn/>) was then used to determine the overlapping target proteins among the hit-to-lead compounds. The shared protein targets were further analyzed to explore their interactions using STRING database version 12.0 (<https://string-db.org/>).<sup>29</sup> Finally, a network hub analysis was performed using Cytoscape 3.10.3 software (<https://cytoscape.org/>) to identify potential key protein targets.<sup>30</sup>

### Enrichment analysis of target protein

Several target protein candidates were evaluated to determine their involvement in specific biological pathways. Pathway enrichment analysis was performed using the web-based tool ShinyGo 0.81 (<https://bioinformatics.sdstate.edu/go/>).<sup>31</sup> Based on the pathway involvement, proteins with significant roles in cancer-related pathways were selected for further investigation. These cancer-associated target proteins were further analyzed to evaluate the genetic influence of the genes encoding them. Genetic alteration analysis was performed using cBioPortal (<https://www.cbioportal.org/>),<sup>32</sup> focusing on the breast cancer cohort as a sample.<sup>33</sup>

Additionally, data mining was conducted using the publicly available GEPIA platform (<http://gepia.cancer-pku.cn/>) to compare the gene expression levels of selected target protein between tumor samples and normal tissues in the breast cancer cohort. Survival analysis was also performed to predict the impact of the target protein on patient outcomes.<sup>34</sup> Finally, a correlation analysis was conducted to assess the relationship between the gene expression levels of the selected target protein and the infiltration of various immune and stromal cells typically present in the tumor microenvironment. Data was retrieved and analyzed using TIMER 2.0 (<http://timer.cistrome.org/>).<sup>35</sup>

### Protein structure validation

After identifying the selected target protein, the 3D structure was retrieved from the RCSB Protein Data Bank (<https://www.rcsb.org/>).<sup>36</sup> The MMP9-inhibitor complex with PDB ID 1GKC was chosen for subsequent molecular docking and molecular dynamics analyses.<sup>37</sup> The quality of the selected protein structures was validated using SAVES v6.1 (<https://saves.mbi.ucla.edu/>) and ProSA-web (<https://prosa.services.came.sbg.ac.at/prosa.php>).<sup>38</sup>

### Molecular docking and dynamics simulation

Before conducting molecular docking and dynamics simulations, the structures of hit-to-lead compounds of *M. citrifolia* were retrieved from the PubChem database (<https://pubchem.ncbi.nlm.nih.gov/>). After completing the chemical structure retrieval and target protein preparation, molecular docking was performed using PyRx 0.8 software (<https://pyrx.sourceforge.io/>).<sup>39</sup> Docking coordinates for the target protein were aligned with the native ligand's binding area, ensuring the same binding region was used for the docking of *M. citrifolia* compounds. In this study, marimastat (CID: 119031), an MMP9 inhibitor, was used as the control drug.<sup>40</sup> Furthermore, molecular dynamics simulations were carried out using YASARA software (<https://www.yasara.org/>) under physiological conditions, including a pH of 7.4, 0.9% NaCl concentration, a temperature of 310 K, a water density of 0.997 g/cm<sup>3</sup>, and a pressure of 1 atm.<sup>41</sup> The molecular docking and dynamics simulation results were visualized using BIOVIA Discovery Studio Visualizer (<https://www.3ds.com>).

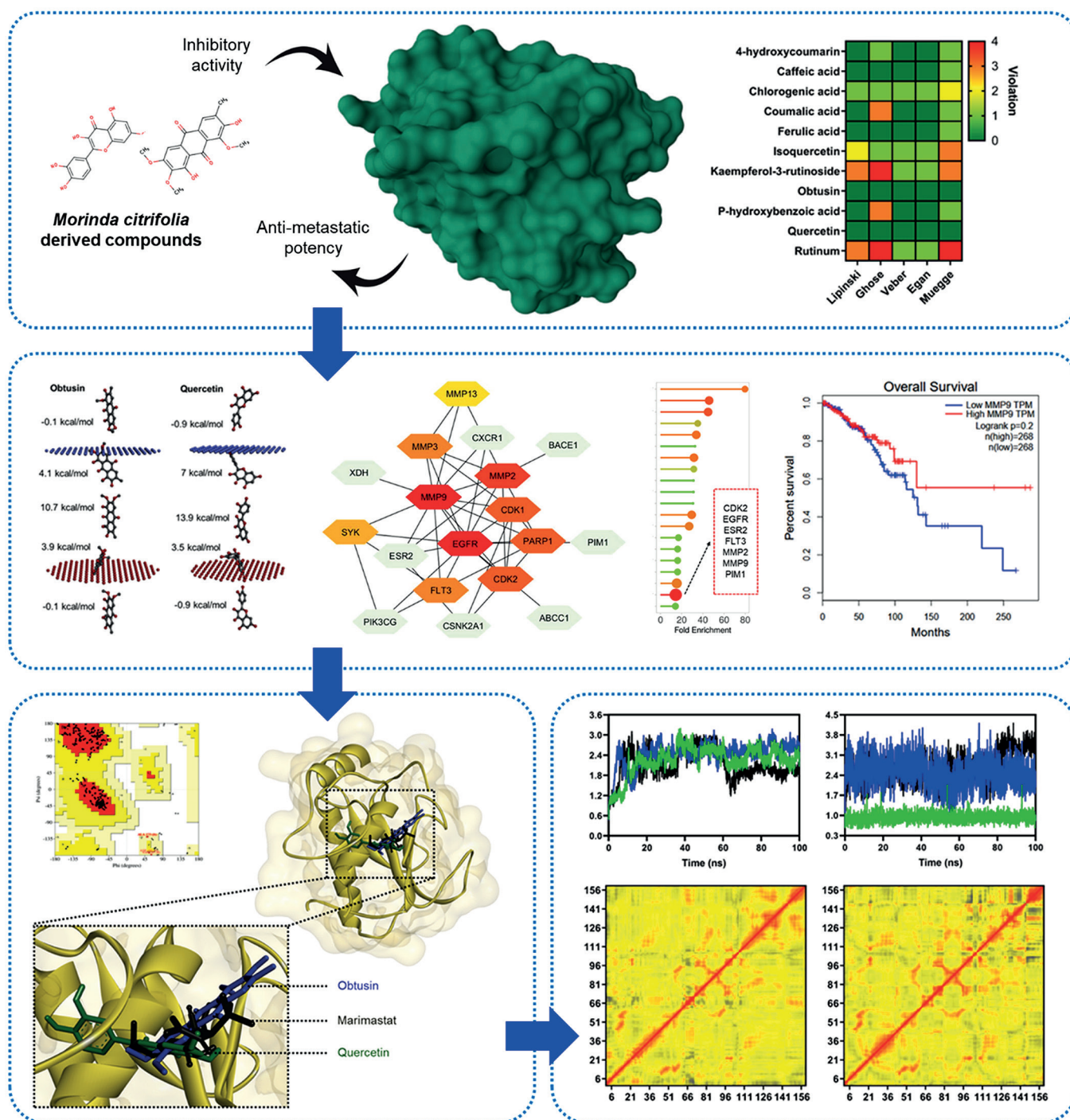


**Figure 1:** Schematic methodology for this study which includes virtual screening, protein selection and enrichment analysis, molecular docking, and molecular dynamics simulation.

## RESULTS AND DISCUSSION

### Drug-likeness screening, toxicity evaluation, biological activity, and membrane permeability prediction

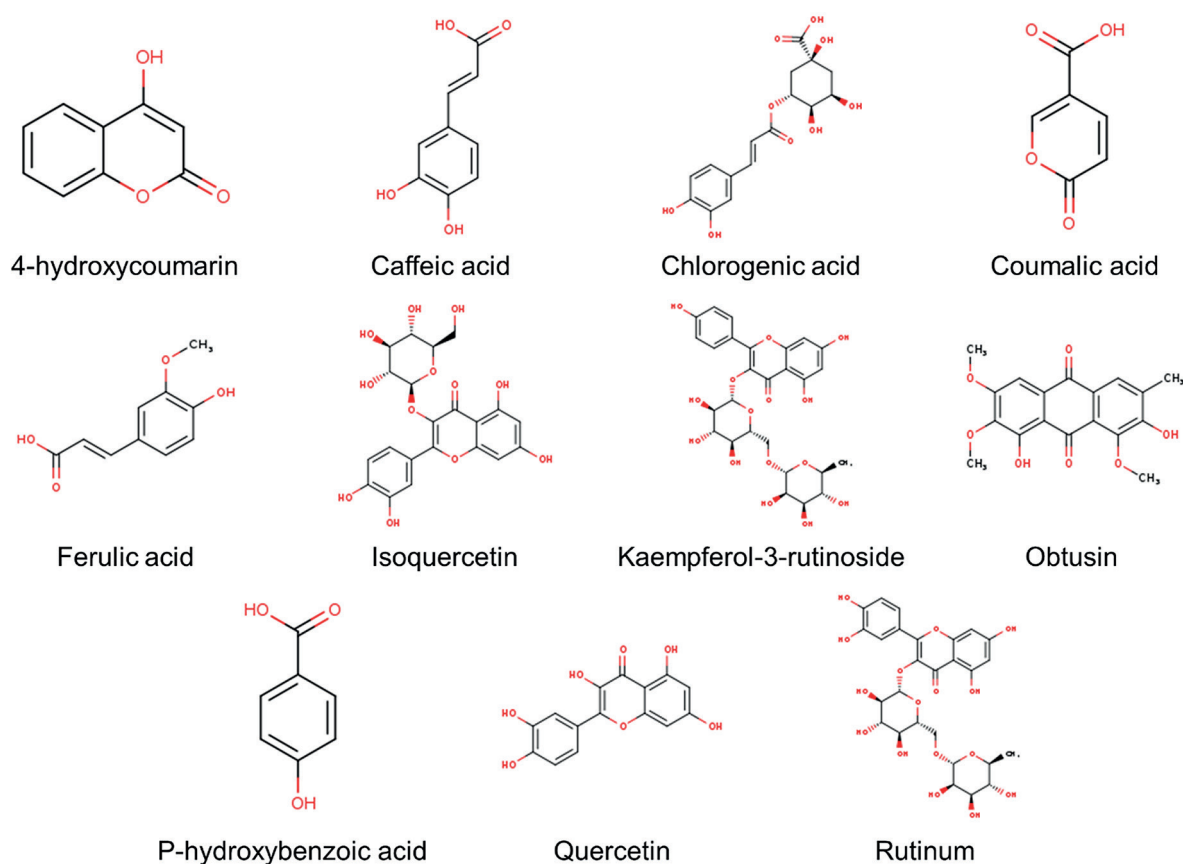
*M. citrifolia* contains a variety of major active compounds, including 4-hydroxycoumarin, caffeic acid, chlorogenic acid, coumalic acid, ferulic acid, isoquercetin, kaempferol-3-rutinoside, obtusin, p-hydroxybenzoic acid, quercetin, and rutinum (Figure 2). These compounds exhibit a wide range of therapeutic properties due to their unique structural and physicochemical characteristics (Table 1). Among these active compounds, virtual screening was conducted to identify those with potential as drug candidates. Virtual screening is a critical step in drug discovery, as it not only enhances the optimization of candidate compounds but also improves time and cost efficiency, thereby accelerating the drug development process.<sup>42</sup> Drug-likeness

screening was the initial step in evaluating the active compounds based on commonly used criteria for determining drug-like properties. These criteria included Lipinski's Rule of Five, Ghose, Veber, Egan, and Muegge rules. Of the eleven compounds evaluated, only two, obtusin and quercetin, met all five drug-likeness criteria (Figure 3A).

Toxicity predictions were subsequently performed on these two hit-to-lead compounds. Several parameters were assessed, including toxicity class prediction, predicted LD50 values, and the probability of organ toxicity induced by the tested compounds (Figure 3B). The results revealed that quercetin exhibited higher toxicity levels compared to obtusin. However, interestingly, both compounds showed minimal potential for causing excessive toxicity in organs based on the evaluated parameters. Toxicity evaluation is a crucial aspect of drug development, as it helps to mitigate adverse effects and optimize the safety profile of potential drug candidates. Conducting toxicity

**Table 1:** Chemicals properties of *Morinda citrifolia* L. bioactive compounds.

Compounds	Molecular weight (g/mol)	Number of H-bond acceptors	Number of H-bond donors	Molar Refractivity	TPSA (Å <sup>2</sup> )
4-hydroxycoumarin	162.14	3	1	44.51	50.44
Caffeic acid	180.16	4	3	47.16	77.76
Chlorogenic acid	354.31	9	6	83.5	164.75
Coumalic acid	140.09	4	1	31.94	67.51
Ferulic acid	194.18	4	2	51.63	66.76
Isoquercetin	464.38	12	8	110.16	210.51
Kaempferol-3-rutinoside	594.52	15	9	139.36	249.2
Obtusin	344.32	7	2	88.24	102.29
P-hydroxybenzoic acid	138.12	3	2	35.42	57.53
Quercetin	302.24	7	5	78.03	131.36
Rutinum	610.52	16	10	141.38	269.43

**Figure 2:** Chemical structure of *Morinda citrifolia* L. bioactive compounds.

evaluations *in silico* offers significant advantages in terms of cost and labor, as well as reducing reliance on animal models.<sup>43,44</sup>

Further analysis involved predicting the biological activity of the two hit-to-lead compounds to assess their potential, particularly in the context of cancer. Several parameters associated with the hallmarks of cancer progression were evaluated to compare the dominant biological activities of each compound (Figure 3C). The results indicated that quercetin exhibited a more pronounced anticancer profile compared to obtusin, as evidenced by higher Pa values across the measured parameters. In biological activity prediction, a Pa value closer to 1 indicates a higher likelihood of the compound exhibiting the predicted activity.<sup>45</sup>

Finally, virtual screening was extended to evaluate the ability of the compounds to penetrate the lipid bilayer membrane. This property is vital in drug discovery, as a good drug candidate must exhibit high membrane permeability to ensure optimal therapeutic effects.<sup>46,47</sup> The membrane permeability prediction data showed that both obtusin and

quercetin could effectively penetrate the lipid bilayer membrane (Figure 3D). In summary, the virtual screening highlights the potential of obtusin and quercetin as promising drug candidates due to their drug-likeness properties, minimal toxicity risks, notable biological activities, and favorable membrane permeability.

### Target protein determination

Combining the predicted target proteins of the two hit-to-lead compounds, obtusin and quercetin, a total of 20 target proteins were identified (Figure 4A). A degree hub analysis was performed on these target proteins to determine the number of interactions (Figure 4B). The results of the network pharmacology analysis revealed that MMP9 and epidermal growth factor receptor (EGFR) ranked the highest, indicating that these two proteins play significant roles and have substantial influence on other proteins.

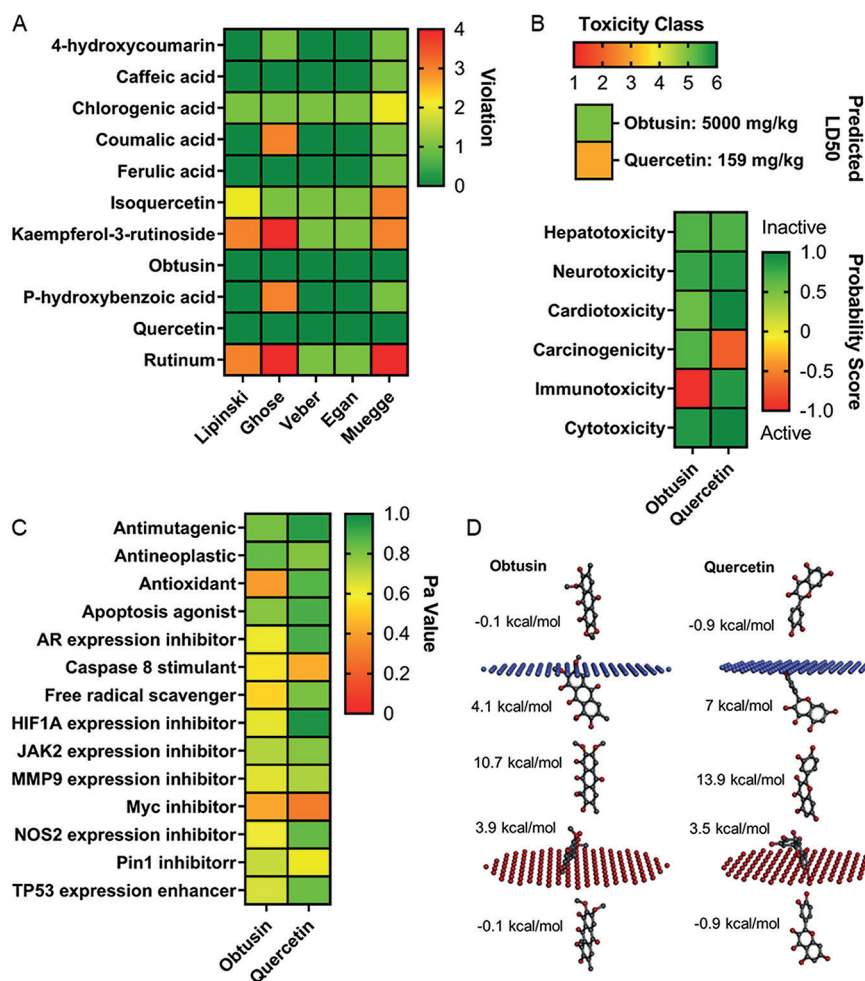


**Figure 3:** Virtual screening of *Morinda citrifolia* L. bioactive compounds. A). Drug-likeness screening. B). Toxicity prediction. C). Biological activity prediction. D). Membrane permeability prediction.

According to previous studies, the network hub approach is commonly used to identify key proteins in biological pathways, characterized by having the most and most significant connections. Moreover, network hubs are frequently employed to determine potential drug targets and analyze the molecular mechanisms of diseases.<sup>48,49</sup> In this context, MMP9 and EGFR are predicted to have crucial roles and hold potential as promising candidates for drug development.

Subsequently, pathway enrichment analysis was conducted to identify the biological pathways associated with the 20 target proteins (Figure 5A). The results showed that these proteins are involved in various pathways. Notably, several target proteins, including cyclin-dependent kinase 2 (CDK2), EGFR, estrogen receptor beta (ESR2), FMS-like tyrosine kinase 3 (FLT3), MMP2, MMP9, and proto-oncogene, serine/threonine kinase (PIM1), are part of the pathways in cancer. These seven protein-coding genes were further evaluated for their genetic alteration percentages in cases of breast invasive cancer. Interestingly, MMP9 exhibited the highest genetic alteration rate, at 6%, compared to other target proteins (Figure 5B). Based on network pharmacology, pathway enrichment, and genetic alteration analyses, MMP9 emerges as a potential target for obtusin and quercetin in drug development for breast invasive cancer. Target protein screening is critical in drug discovery studies as it helps optimize the specificity of compounds being tested, ultimately advancing the drug development process.<sup>50</sup>

### Enrichment and immune infiltration analysis

Further enrichment analysis was conducted on MMP9 as the target protein in this study. Publicly available data revealed that MMP9 expression is significantly higher in tumor samples compared to normal samples within the breast cancer cohort (Figure 6A).

Interestingly, survival analyses showed that high MMP9 expression is associated with poorer overall survival and disease-free survival outcomes compared to low MMP9 expression (Figure 6B). These findings support the potential of MMP9 as a promising target protein for cancer drug development. In the context of cancer, MMP9 plays a pivotal role in driving cancer progression, primarily by facilitating metastasis in various types of cancers.<sup>51</sup>

Moreover, MMP9 expression significantly influences the infiltration levels of various immune and stromal cells, which are key components of the tumor microenvironment. Correlation analysis indicated that MMP9 expression positively correlates with the infiltration of monocytes, macrophages, neutrophils, and regulatory T cells while negatively correlated with myeloid-derived suppressor cells and cancer-associated fibroblasts. Interestingly, MMP9 expression showed no significant correlation with the infiltration of cytotoxic T cells and natural killer cells (Figure 7). The tumor microenvironment is closely linked to poor prognosis and cancer progression in patients.<sup>52,53</sup> Therefore, correlation analysis is crucial to understanding how gene expression impacts the infiltration of various immune and stromal cells that constitute the tumor microenvironment. This information can provide valuable insights into potential therapeutic strategies targeting MMP9 in cancer treatment.

### Protein structure validation

Structure validation was performed before conducting molecular docking and dynamics simulation to evaluate the effects of hit-to-lead compounds on the MMP9 protein. Ramachandran plot assessment revealed that 90.4% of residues were located in the most favored regions (Figure 8A). Subsequently, ProSA-web analysis indicated a

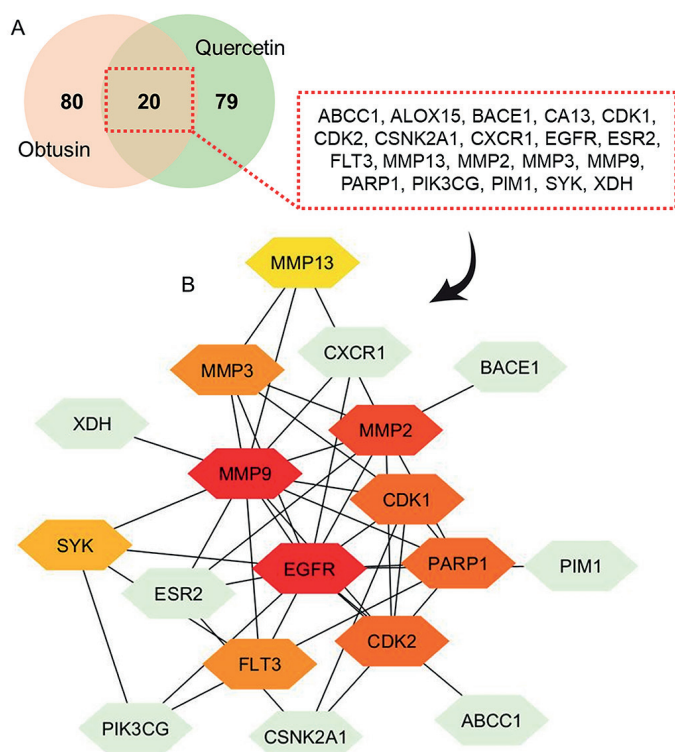


**Figure 4:** Target protein intersection and network pharmacology. A). The intersection of common target proteins between obtusin and quercetin. B). Protein-protein interaction from selected proteins.



**Figure 5:** Pathways enrichment and genetic alteration analysis. A). Pathways enrichment analysis of selected proteins. B). Genetic alteration of selected proteins in breast invasive carcinoma cohort retrieved from public data.

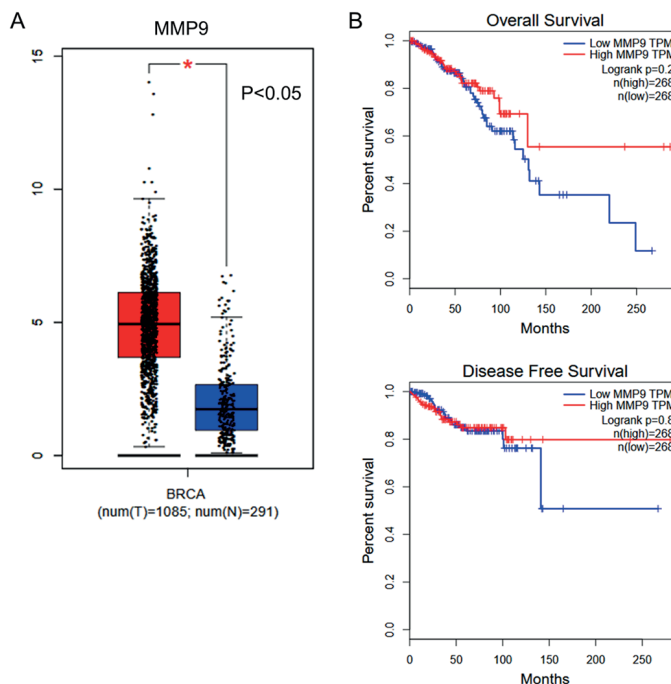


**Figure 6:** Enrichment analysis. A). Gene expression of MMP9 gene in tumor and normal sample of breast cancer patient cohort from public data. B). Prognosis estimation related to the MMP9 expression.

Z-score of -5.49, suggesting high structural quality, as evidenced by the predominance of negative values in the knowledge-based energy profile (Figure 8B). Lastly, VERIFY 3D and ERRAT plot assessments demonstrated excellent structural quality, with values of 93.97% and 80.205%, respectively (Figures 8C and 8D). Following that, the target protein was obtained from a public database, and structure validation is crucial to ensure the structure accurately represents its biological conformation and to identify any structural errors. Additionally, a validated structure provides reliable information, enabling other researchers to reproduce the study and potentially improve upon it.<sup>54</sup> In this scenario, the protein target is deemed to be structurally reliable.

### Molecular docking and dynamics simulation

Molecular docking was performed to evaluate the potential of the hit-to-lead compounds to bind with the target protein. The results showed that quercetin exhibited a binding affinity value of -9.0 kcal/mol, which is more favorable compared to obtusin and the control drug, Marimastat, both of which displayed a binding affinity of -7.5 kcal/mol (Figure 9A). Interestingly, the binding regions of the hit-to-lead compounds were similar to those of the control drug within the same cavity (Figure 9B). These findings suggest that, besides having a more favorable binding affinity, the hit-to-lead compounds have comparable potential to the control drug in interacting with the target protein, indicating their therapeutic potential as MMP9 inhibitors and a similar mechanism of action with the control drug. Molecular docking is a widely used approach to evaluate a compound's potential to interact with a target protein. Lower binding affinity values indicate a higher likelihood of the compound binding to the target protein, making it a key reference point for further drug development.<sup>55,56</sup>

A molecular dynamics simulation was conducted to evaluate further the interaction between the ligand and the target protein. This approach provides insights into the stability of the ligand-protein interaction over time. The data revealed changes in position and conformation during the simulation for both the ligand (Figure 10) and the protein (Figure 11). Although some conformational change is observed among the compounds, they are still primarily held by

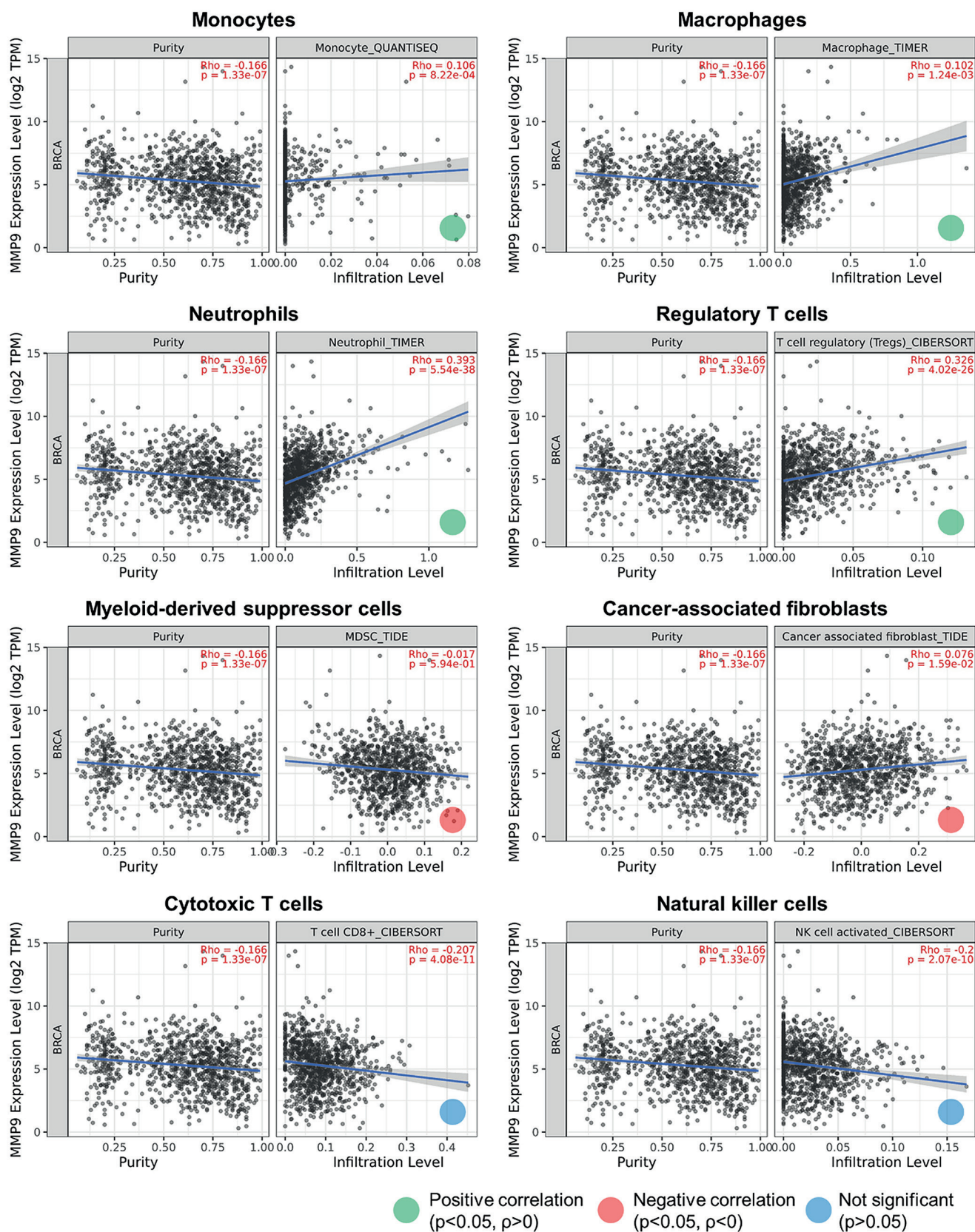


**Figure 7:** The correlation analysis between the MMP9 gene expressions in breast cancer patient cohort with the tumor microenvironment component infiltration using public data.

their backbone, preventing any dramatic conformational changes. The same is the case with the MMP9 protein structure. It maintains its shape during simulation when coupled with quercetin, obtusin, and Marimastat. These changes suggest that ligand-protein interactions are influenced by various factors, including the involvement of different types of chemical interactions such as hydrogen bonding, van

der Waals forces, electrostatic, and dipole-dipole interactions from within and around the complex. These interactions can alter positions and functional characteristics, impacting the ligand's therapeutic properties and influencing protein responses.<sup>57</sup>

Several key parameters were assessed during the molecular dynamics simulation, including root mean square deviation (RMSD)

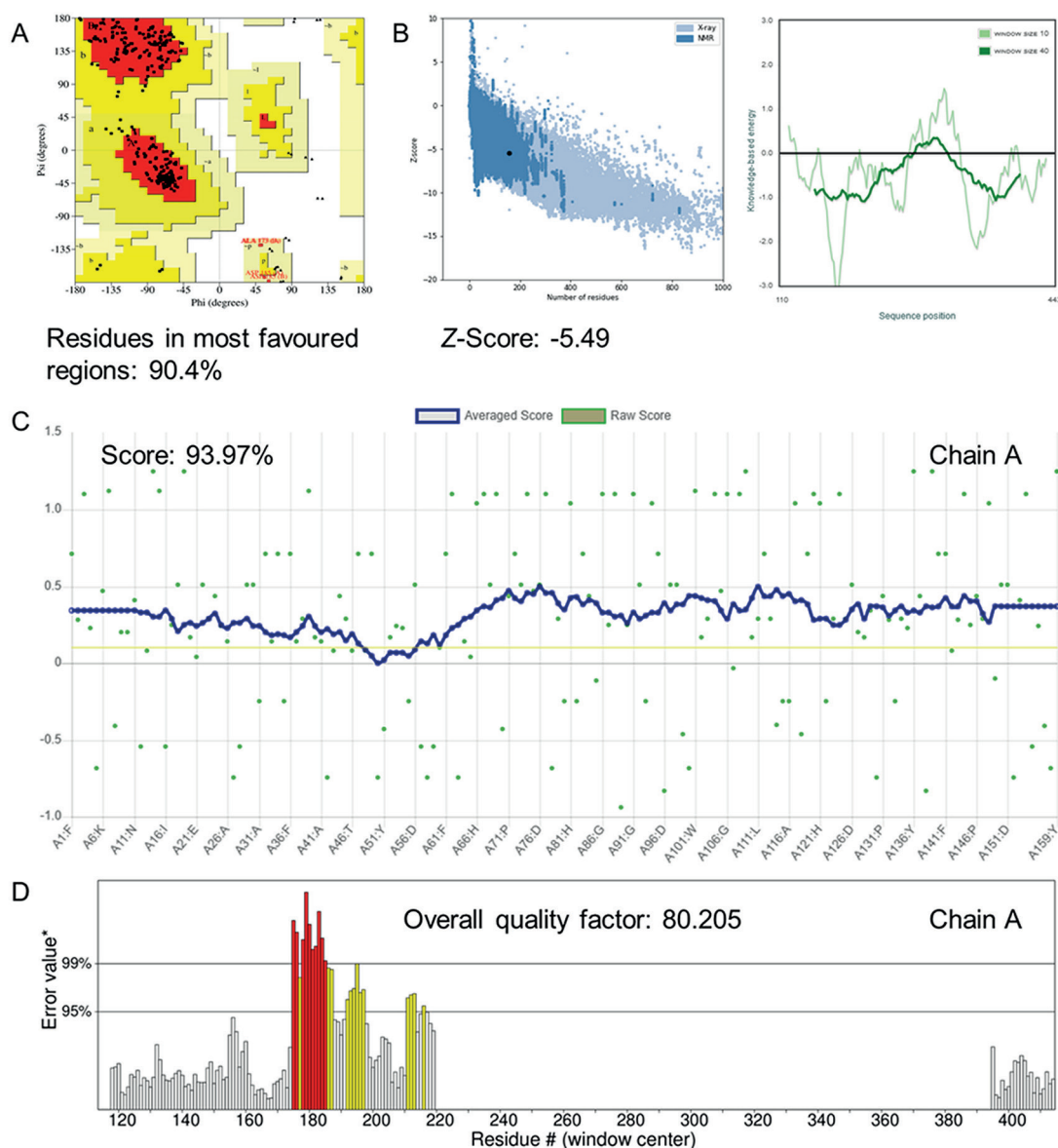


**Figure 8:** MMP9 protein structure validation. A). Ramachandran plot assessment by SAVES. B). Protein structure analysis by ProSA-web. C). VERIFY 3D plot assessment by SAVES. D). ERRAT plot assessment by SAVES.

of the backbone, RMSD of ligand movement, RMSD of ligand conformation, root mean square fluctuation (RMSF), the radius of gyration, solvent accessible surface area (SASA), H-bond interactions, binding energy plots, and dynamic cross-correlation matrix (DCCM) (Figures 12 and 13). The results showed similar trends between complexes for all parameters. The RMSD results show that all the compounds may fluctuate up to 40 ns before stabilizing between 1.0-3.0Å, showcasing substantial conformational shifts throughout the simulation. Interestingly, the ligand movement plot shows that quercetin exhibits an exceptionally stable plot around 1.0Å, while the other two fluctuated around 1.5-4.2Å. Ligand conformation plot also confirms the results from Figure 10, which shows both hit-to-lead compounds have extraordinarily stable conformation with 0.5 and 1.0Å for quercetin and obtusin, respectively, even when compared to the control. The RMSF plot further confirmed the results from Figures 9 and 10, which indicates that all compounds occupy the same binding cavity. Higher RMSF for certain residues in the presence of hit-to-target compounds may indicate that these ligands induce more flexibility in the active site region, potentially affecting the protein's ability to adopt the optimal conformation for its activity.

As we examined the ligand-protein complexes throughout the simulation, the overall protein structure remains consistently compact and doesn't undergo significant unfolding or expansion upon binding

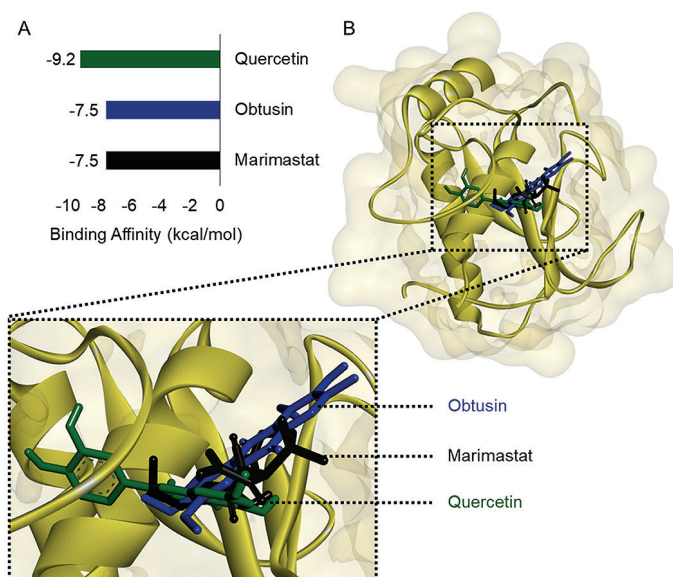


**Figure 9:** Molecular docking results of ligands against the target protein. A). Binding affinity scores. B). The three-dimensional visualization of MMP9-ligand complex.

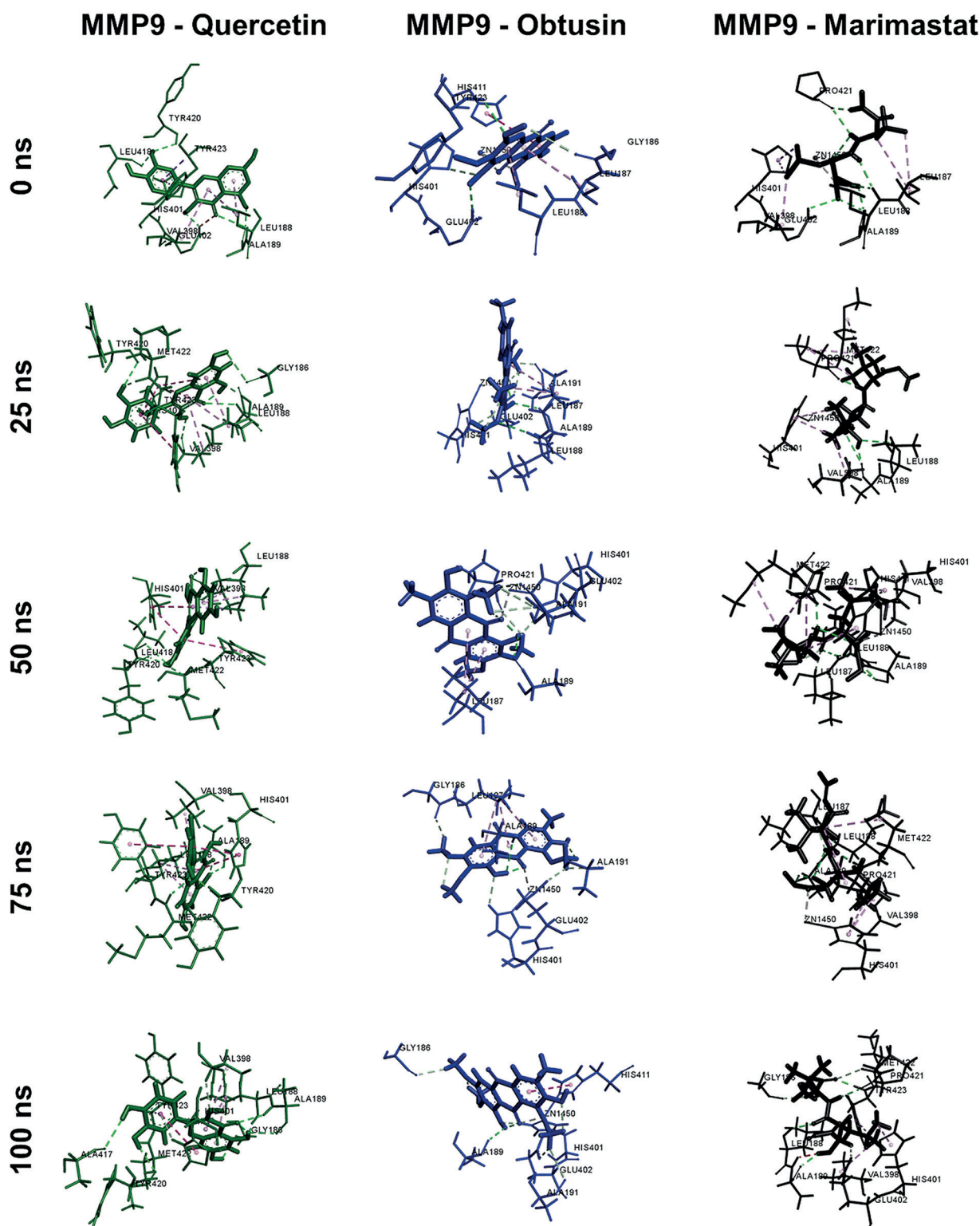


**Figure 10:** Ligand motion and conformational shift during dynamics simulation of quercetin, obtusin, and marimastat against the target protein.

any ligands. There is some degree of fluctuation in the first 40 ns of simulations, but it does not indicate any major conformation changes in the protein. These results were also confirmed by the SASA plot, further supporting the notion that the ligand interaction does not induce significant changes in the conformation.

The DCCM results show an interesting pattern. The distinct pattern of correlated motions observed in the MMP9-marimastat complex suggests that marimastat may stabilize specific conformations or induce a particular dynamic state crucial for its inhibitory activity, which might involve restricting certain movements necessary for catalysis. On the other hand, the weaker and less-defined correlations

in both hit-to-lead compound complexes suggest that these ligands have a less pronounced effect on the protein's overall dynamics.

Obtusin exhibited a more favorable value for the binding energy value than the others. At the same time, quercetin and the control drug showed similar trends with higher average binding energy values than obtusin. However, quercetin demonstrated more significant ligand movement and conformation stability, with lower average RMSD values than obtusin and the control drug, indicating superior stability over the 100 ns simulation period. These findings highlight the distinct potential of the compounds, particularly quercetin, in achieving stable and effective interactions with MMP9.

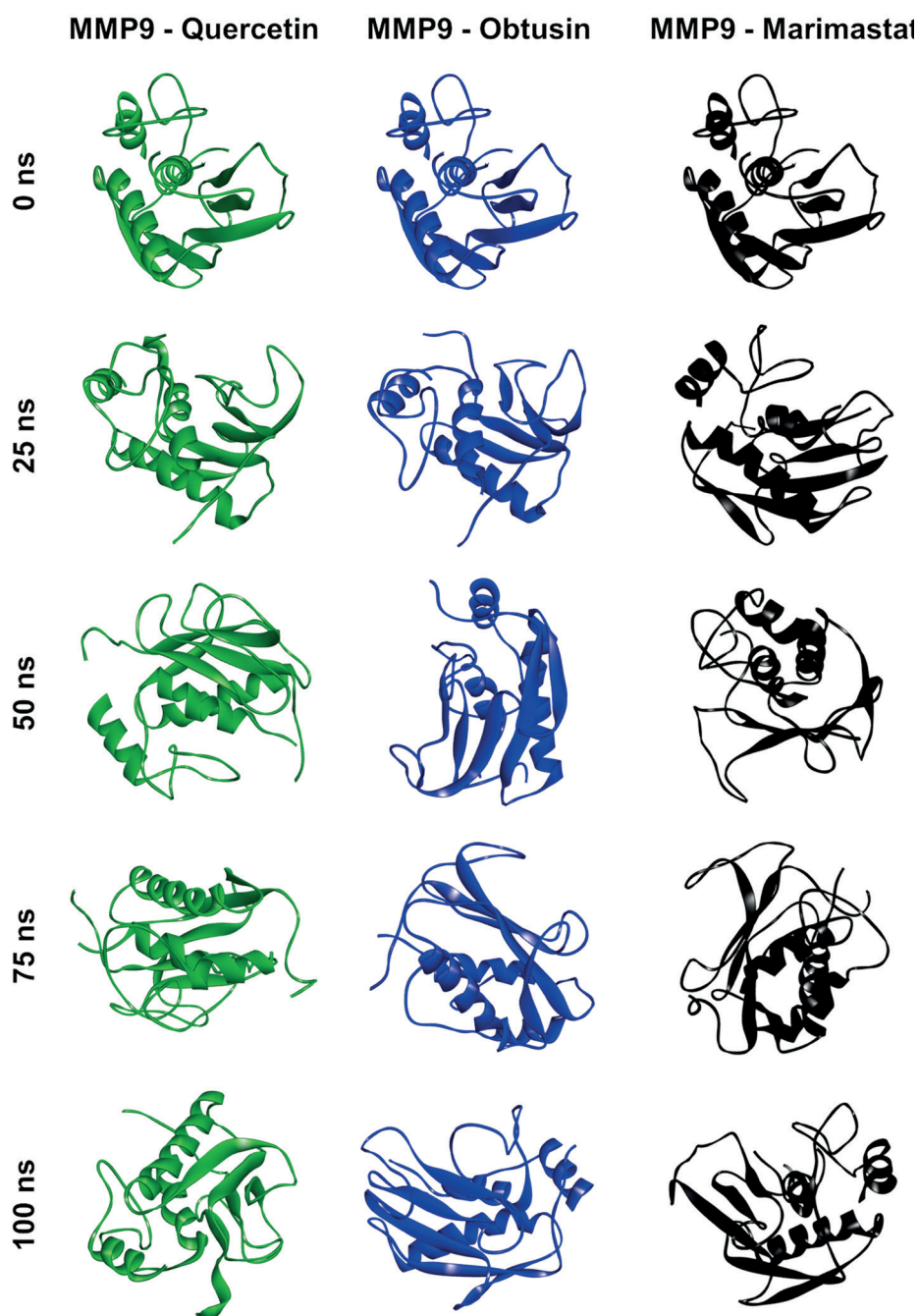


**Figure 11:** Protein motion and shift during dynamics simulation of quercetin, obtusin, and marimastat against the target protein.

Passing the drug-likeness criteria threshold is one of the key standards for identifying potential drug candidates. These criteria include having a molecular weight  $\leq 500$  Daltons, hydrogen bond donors  $\leq 5$ , hydrogen bond acceptors  $\leq 10$ , lipophilicity  $\leq 5$ , minimal toxicity effects, and high membrane permeability.<sup>58–60</sup> Quercetin, which was shown to have favorable drug-likeness properties with minimal toxicity effects and promising biological activity as an anti-cancer agent, has demonstrated a strong potential as an anti-cancer drug candidate compared to obtusin and the control drug. There have been numerous reports on the anti-cancer potential of quercetin. For instance, quercetin has been shown to induce pro-apoptotic effects in various cancer types.<sup>61</sup> Moreover, it can inhibit the proliferation and invasion of human breast cancer cells by up-regulating miR-146a.<sup>62</sup> Additionally, quercetin induces cell cycle arrest and promotes cell death in cancer stem cells of human colorectal HT29 cancer cell lines.<sup>63</sup> It also regulates the miR-16/HOXA10 axis in oral cancer, thereby inhibiting cell viability, invasion, and migration.<sup>64</sup> In the case of human metastatic osteosarcoma, quercetin reduces invasion,

adhesion, proliferation, and migration.<sup>65</sup> Interestingly, studies on lung cancer cell lines (A549 cells) revealed that quercetin exerts its anti-cancer effects by reducing the phosphorylation of IKK $\beta$  and I $\kappa$ B, decreasing the expression of NF- $\kappa$ B and MMP-9.<sup>66</sup>

The MMP9, identified as a potential target for quercetin, plays a significant role in cancer progression. Its increased expression strongly correlates with poor prognosis in cancer patients, making it a promising biomarker target in cancer therapy. Studies have reported that MMP9 regulates key processes such as cell migration, epithelial-to-mesenchymal transition, enhanced cancer cell survival, angiogenesis promotion, and modulation of the tumor microenvironment.<sup>51</sup> For example, MMP9 mRNA and protein levels have been found to be significantly elevated in breast cancer cell lines. Similarly, clinical studies have demonstrated that MMP9 expression is higher in breast cancer tissues compared to normal tissues, further linking its elevated expression to poor patient prognosis.<sup>67</sup> Interestingly, MMP9 also promotes the activation of IL-1 $\beta$  and TGF- $\beta$ . The presence of these molecules acts as a bridge between inflammation and cancer, highlighting the multifaceted role of MMP9

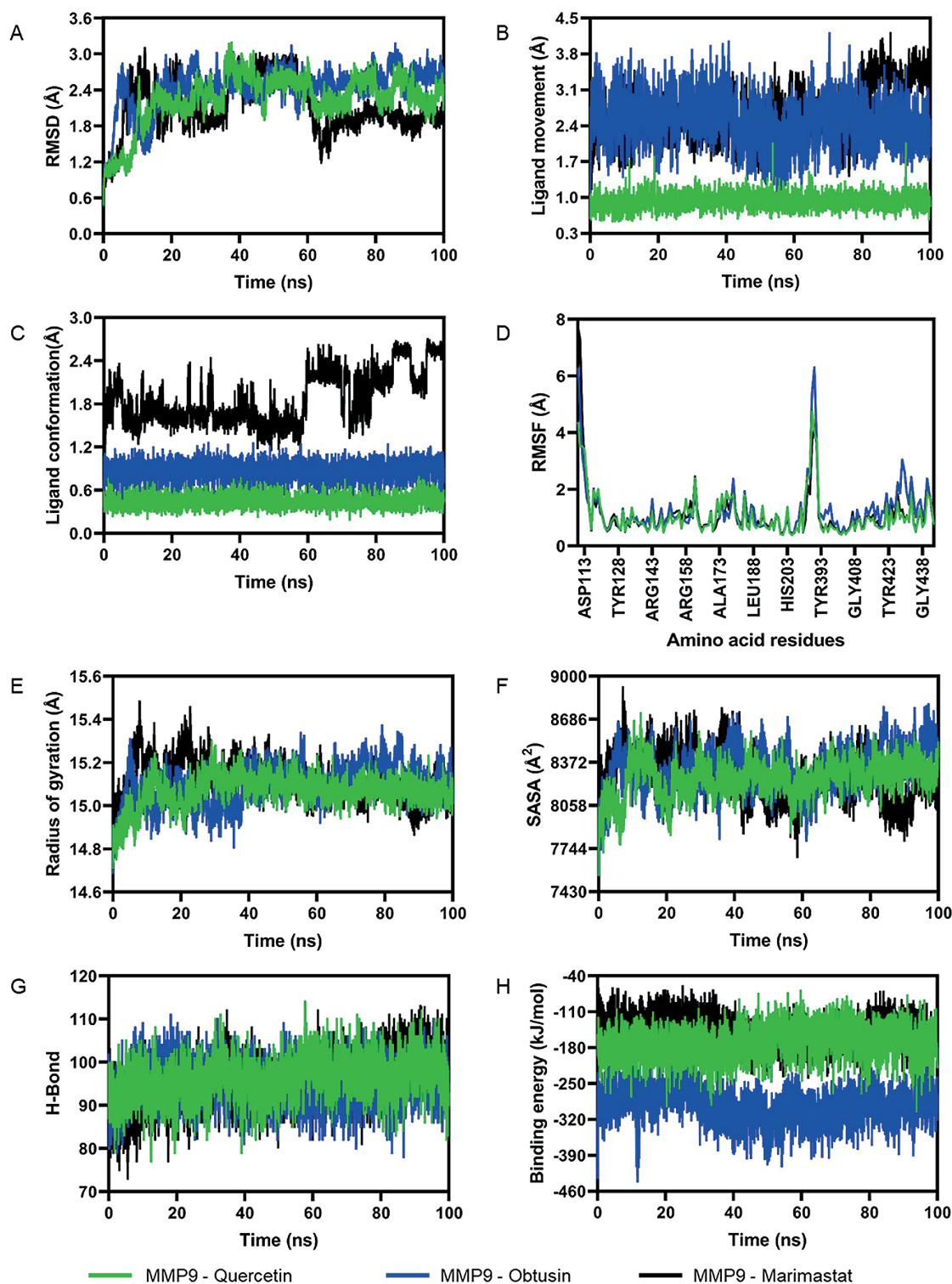


**Figure 12:** Molecular dynamics simulations of quercetin, obtusin, and marimastat against the target protein, MMP9. A). RMSD of backbone plot. B). RMSD of ligand movement plot. C). RMSD of ligand conformation plot. D). RMSF plot. E). Radius gyration plot. F). SASA plot. G). H-bond interaction plot. H). Binding energy plot.

in tumor progression and inflammation-driven carcinogenesis.<sup>68</sup> On top of that, a recent study demonstrated that MMP9 is related to immune infiltration in pan-cancer studies.<sup>69</sup>

Structurally, the MMP9 consist of several key structural domains, including the catalytic domain and the hydrophobic S1' pocket structure. The catalytic domain centered on the zinc-binding motif (His401, His405, His411) and flanked by the hydrophobic S1 pocket (Leu188, Val398, Tyr423), which is crucial for substrate selection, drives cancer progression through multifaceted proteolytic and signalling mechanisms.<sup>70-73</sup> By degrading structural ECM components like collagen IV and laminin, MMP-9 facilitates metastatic dissemination. At the

same time, its cleavage of latent precursors such as VEGF-A and TGF- $\beta$  activates angiogenic signalling, promoting tumor vascularization. The catalytic core reprograms the immune microenvironment by truncating CXCL12 to impair T-cell infiltration and solubilise IL-2R $\alpha$  to blunt lymphocyte activation, while autolytic activation perpetuates protease cascades. It also mobilizes growth factors like HB-EGF and IGF-1 through IGFBP-3 cleavage, fostering tumor survival and therapy resistance, and exhibits context-dependent duality in apoptosis regulation via angiostatin generation or FasL inactivation.<sup>51,74</sup>

The docking and molecular dynamic results showed that the hit-to-lead compounds and the control have interacted with the same

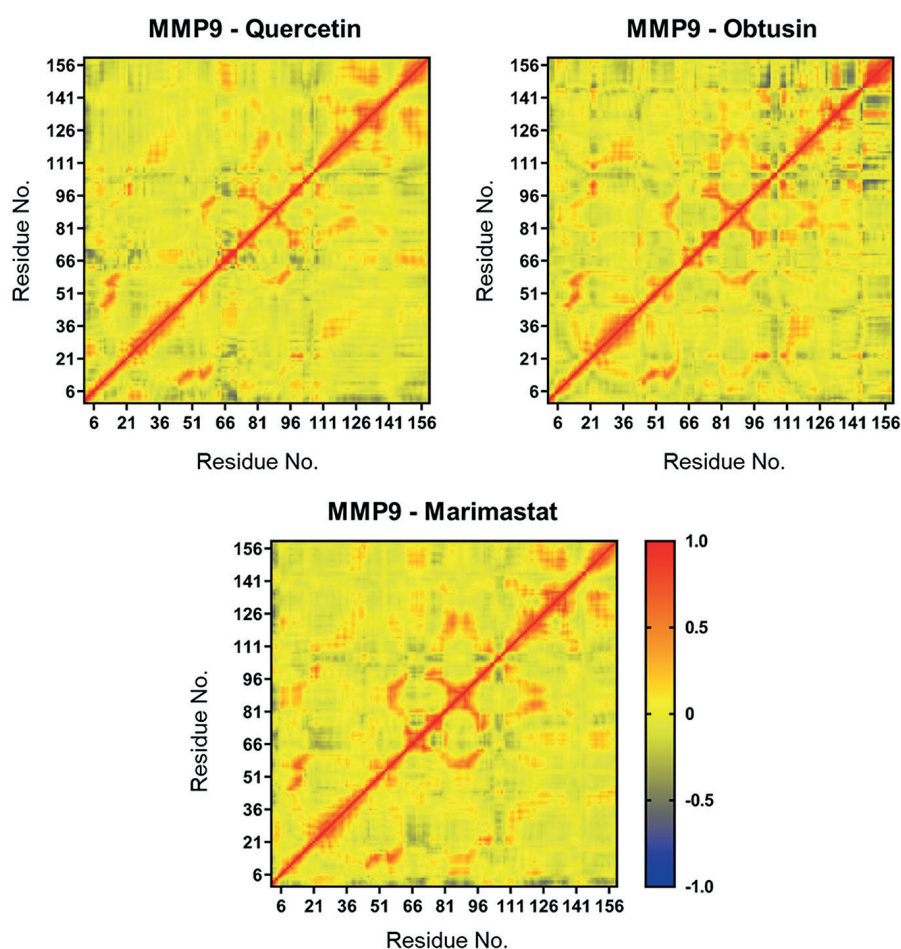


**Figure 13:** Dynamics cross-correlation matrix analysis of MMP9-ligand complex.

binding cavity along the simulation duration, specifically with the critical residues along the catalytic domain in the zinc-binding motif, as well as the main catalytic base (Glu402). It is generally thought that Marimastat's inhibition of MMP-9 hinges on its hydroxamate group binding to the catalytic zinc ion, blocking substrate hydrolysis, mimicking its native ligand  $N^2$ -[(2R)-2-[[Formyl(hydroxy)amino]methyl]-4-methylpentanoyl]-N,3-dimethyl-L-valinamide also known as NFH.<sup>75</sup> Comparative analyses of MMP-9 crystallographic structures reveal that marimastat binds this cavity by coordinating the catalytic zinc ion and forming hydrogen bonds with Ala189 and Leu187.<sup>73</sup> This may suggest that both hit-to-lead compounds possess similar activity and action mechanisms as marimastat and native ligands through direct competitive inhibition. Other research suggests that quercetin's catechol moiety enables chelation of the catalytic zinc ion with enhanced affinity due to its polypharmacological scaffold but also depends on its hydroxylation pattern.<sup>76,77</sup> Although obtusin was shown to interact with the same cavity as quercetin and Marimastat, other research suggests that it is not directly involved in the catalytic activity of the catalytic core. Due to its lower polarity, obtusin does not directly chelate the zinc ion; instead, it displaces the water molecule essential for zinc-mediated catalysis and disrupts the S1 pocket. This disruption leads to a remodeling of the binding site cavity, rendering it unable to interact with the designated ligand for downstream signaling pathways.<sup>78,79</sup>

## CONCLUSION

In this study, we highlight the role of the major compounds of *M. citrifolia* L., a plant widely grown in tropical regions, as potential cancer drug candidates. Using a multiple and integrative *in silico* approach, we have demonstrated that *M. citrifolia* L. may exert anti-metastatic effects by targeting MMP-9, a protein associated with metastasis. Quercetin and obtusin inhibit MMP-9 through

distinct yet complementary mechanisms. While quercetin employs zinc chelation and multi-point hydrogen bonding, obtusin relies on cavity remodeling and allosteric modulation. Both compounds share Marimastat's binding site but diverge in their interaction and mechanism of action, offering opportunities for both to be deployed as therapeutic agents targeting metastasis. The data obtained from this investigation is preliminary findings and provides valuable insights for developing drug candidates to mitigate metastasis, which is commonly observed in advanced stages of cancer. The strategy we have used not only highlights the compounds most likely responsible for the plant's traditional therapeutic use but also increases the relevance of the findings for future drug discovery and development. Further experimental research in *in vitro* and *in vivo* is needed to confirm these findings.

## ACKNOWLEDGEMENTS

The authors thank Universitas Negeri Malang for financial support this study.

## CREDIT AUTHORSHIP CONTRIBUTION STATEMENT

W.E.P. and A.H. contributed to conceptualization, methodology, software, formal analysis, data curation, and writing—original draft. D.W., H.L., M.E.H., and S.S. contributed to conceptualization, formal analysis, data curation, and writing—review and editing. All authors have reviewed and approved the final version of the manuscript for publication.

## DECLARATION OF COMPETING OR FINANCIAL INTERESTS

The authors report no conflict of interest in this study.

## ORCID IDS

Wira Eka Putra: <https://orcid.org/0000-0003-4831-3869>  
Arief Hidayatullah: <https://orcid.org/0000-0003-1929-3635>  
Diana Widiastuti: <https://orcid.org/0000-0001-6844-3906>  
Hary Isnanto: <https://orcid.org/0000-0002-2519-621X>  
Muhammad Fikri Heikal: <https://orcid.org/0000-0002-4672-8107>  
Sustiprijatno Sustiprijatno: <https://orcid.org/0000-0001-8623-8471>

## REFERENCE

1. Sha R, Kong XM, Li XY, Wang YB. Global burden of breast cancer and attributable risk factors in 204 countries and territories, from 1990 to 2021: Results from the Global Burden of Disease Study 2021. *Biomark Res.* 2024;12(1):87. <https://doi.org/10.1186/s40364-024-00631-8>.
2. Arnold M, Morgan E, Rumgay H, Mafra A, Singh D, Laversanne M, Vignat J, Gralow JR, Cardoso F, Siesling S, Soerjomataram I. Current and future burden of breast cancer: Global statistics for 2020 and 2040. *Breast.* 2022;66:15–23. <https://doi.org/10.1016/j.breast.2022.08.010>.
3. Łukasiewicz S, Czezelewski M, Forma A, Baj J, Sitarz R, Stanisławek A. Breast cancer—Epidemiology, risk factors, classification, prognostic markers, and current treatment strategies—An updated review. *Cancers (Basel).* 2021;13(17):4287. <https://doi.org/10.3390/cancers13174287>.
4. Park M, Kim D, Ko S, Kim A, Mo K, Yoon H. Breast cancer metastasis: Mechanisms and therapeutic implications. *Int J Mol Sci.* 2022;23(12):6806. <https://doi.org/10.3390/ijms23126806>.
5. Fares J, Fares MY, Khachfe HH, Salhab HA, Fares Y. Molecular principles of metastasis: A hallmark of cancer revisited. *Signal Transduct Target Ther.* 2020;5(1):28. <https://doi.org/10.1038/s41392-020-0134-x>.
6. Chen J, Yao Y, Gong C, Yu F, Su S, Chen J, Liu B, Deng H, Wang F, Lin L, Yao H, Su F, Anderson KS, Liu Q, Ewen ME, Yao X, Song E. CCL18 from tumor-associated macrophages promotes breast cancer metastasis via P1TPNM3. *Cancer Cell.* 2011;19(4):541–55. <https://doi.org/10.1016/j.ccr.2011.02.006>.
7. Kalali D. The role of the matrix metalloproteinase-9 gene in tumor development and metastasis: A narrative review. *Glob Med Genet.* 2023;10:48–53. <https://doi.org/10.1055/s-0043-1768166>.
8. Wen J, Yin P, Li L, Kang G, Ning G, Cao Y, Gao F, Su Y, Wu Y, Zhang X. Knockdown of matrix metalloproteinase 9 inhibits metastasis of oral squamous cell carcinoma cells in a zebrafish xenograft model. *Biomed Res Int.* 2020;2020:4350783. <https://doi.org/10.1155/2020/4350783>.
9. Wang Y, Jiao L, Qiang C, Chen C, Shen Z, Ding F, Lv L, Zhu T, Lu Y, Cui X. The role of matrix metalloproteinase 9 in fibrosis diseases and its molecular mechanisms. *Biomed Pharmacother.* 2024;171:116116. <https://doi.org/10.1016/j.biopha.2023.116116>.
10. Kochumon S, Al-Sayyar A, Jacob T, Bahman F, Akhter N, Wilson A, Sindhu S, Hannun YA, Ahmad R, Al-Mulla F. TGF- $\beta$  and TNF- $\alpha$  interaction promotes the expression of MMP-9 through H3K36 dimethylation: Implications in breast cancer metastasis. *Front Immunol.* 2024;15:1430187. <https://doi.org/10.3389/fimmu.2024.1430187>.
11. Shan L, Wang F, Zhai D, Meng X, Liu J, Lv X. Matrix metalloproteinases induce extracellular matrix degradation through various pathways to alleviate hepatic fibrosis. *Biomed Pharmacother.* 2023;161:114472. <https://doi.org/10.1016/j.biopha.2023.114472>.
12. Rashid ZA, Bardaweel SK. Novel matrix metalloproteinase-9 (MMP-9) inhibitors in cancer treatment. *Int J Mol Sci.* 2023;24:12133. <https://doi.org/10.3390/ijms241512133>.
13. Hariono M, Nuwarda RF, Yusuf M, Rollando R, Jenie RI, Al-Najjar B, Julianus J, Putra KC, Nugroho ES, Wisnumurti YK, Dewa SP, Jati BW, Tiara R, Ramadani RD, Qodria L, Wahab HA. Arylamide as potential selective inhibitor for matrix metalloproteinase 9 (MMP9): Design, synthesis, biological evaluation, and molecular modeling. *J Chem Inf Model.* 2020;60(1):349–59. <https://doi.org/10.1021/acs.jcim.9b00630>.
14. Kalva S, Agrawal N, Skelton AA, Saleena LM. Identification of novel selective MMP-9 inhibitors as potential anti-metastatic lead using structure-based hierarchical virtual screening and molecular dynamics simulation. *Mol Biosyst.* 2016;12:2519–31. <https://doi.org/10.1039/c6mb00066e>.
15. Singh VK, Rajak N, Gupta PK, Mahapatra AK, Singh AK, Giri R, Garg N. Targeting matrix metalloproteinase-9 (MMP9) in prostate cancer: A computational study on natural product-derived novel potential inhibitors. *Future J Pharm Sci.* 2025;11:86. <https://doi.org/10.1186/s43094-025-00838-y>.
16. Kalva S, Azhagiya Singam ER, Rajapandian V, Saleena LM, Subramanian V. Discovery of potent inhibitor for matrix metalloproteinase-9 by pharmacophore-based modeling and dynamics simulation studies. *J Mol Graph Model.* 2014;49:25–37. <https://doi.org/10.1016/j.jmgl.2013.12.008>.
17. Vo HVT, Patton GN, Kim SJ, Kim N, Lee HJ. Exploring flavonoids as regulators of MMP-2 and MMP-9 in cancer pathogenesis. *Chem Biol Drug Des.* 2025;105:e70145. <https://doi.org/10.1111/cbdd.70145>.
18. Malekipour MH, Shirani F, Moradi S, Taherkhani A. Cinnamic acid derivatives as potential matrix metalloproteinase-9 inhibitors: Molecular docking and dynamics simulations. *Genomics Inform.* 2023;21:e9. <https://doi.org/10.5808/gi.22077>.
19. Atanasov AG, Zotchev SB, Dirsch VM, International Natural Product Sciences Taskforce, Supuran CT. Natural products in drug discovery: Advances and opportunities. *Nat Rev Drug Discov.* 2021;20:200–16. <https://doi.org/10.1038/s41573-020-00114-z>.
20. Chanthira KH, Lim XY, Mohkiar FH, Suhaimi SN, Shafie NM, Tan TYC. Efficacy and safety of *Morinda citrifolia* L. (Noni) as a potential anticancer agent. *Integr Cancer Ther.* 2022;21:15347354221132848. <https://doi.org/10.1177/15347354221132848>.
21. Ma LD, Lin GB, Yang LB, Cao JL, Wang J, Chen QD, Li WQ, Zhong WJ. *Morinda citrifolia* (Noni) juice suppresses A549 human lung cancer cells via inhibiting AKT/nuclear factor- $\kappa$ B signaling pathway. *Chin J Integr Med.* 2021;27(9):688–95. <https://doi.org/10.1007/s11655-020-3421-y>.
22. Huo X, Sun S, Li K, Zhang J, Wang Y, Gao H, Cao Z, Xu X, Ma G, Liu M. Constituent analysis, laxative activity, and toxicological evaluation of methanol extract of Noni fruit (*Morinda citrifolia* L., Rubiaceae). *Food Chem X.* 2023;20:100925. <https://doi.org/10.1016/j.fochx.2023.100925>.
23. Ali M, Manjula SN, Mohiuddin I, Mruthunjaya K, Shakeel F, Mir SA, Wani SUD. Noni enhances the anticancer activity of cyclophosphamide and suppresses myelotoxicity and hepatotoxicity in tumor-bearing mice. *J Cancer Res Clin Oncol.* 2024;150(4):212. <https://doi.org/10.1007/s00432-024-05734-1>.
24. Daina A, Michielin O, Zoete V. SwissADME: A free web tool to evaluate pharmacokinetics, drug-likeness and medicinal chemistry friendliness of small molecules. *Sci Rep.* 2017;7:42717. <https://doi.org/10.1038/srep42717>.
25. Banerjee P, Kemmler E, Dunkel M, Preissner R. ProTox 3.0: A webserver for the prediction of toxicity of chemicals. *Nucleic Acids Res.* 2024;52(W1):W513–W520. <https://doi.org/10.1093/nar/gkac303>.
26. Filimonov DA, Lagunin AA, Glorizova TA, Rudik AV, Druzhilovskii DS, Pogodin PV, Poroikov VV. Prediction of the biological activity spectra of organic compounds using the PASS online web resource. *Chem Heterocycl Compd.* 2014;50(3):444–457. <https://doi.org/10.1007/s10593-014-1496-1>.
27. Lomize AL, Hage JM, Schnitzer K, Golobokov K, LaFave MB, Forsyth AC, Pogozheva ID. PerMM: A web tool and database for analysis of passive membrane permeability and translocation pathways of bioactive molecules. *J Chem Inf Model.* 2019;59(7):3094–3099. <https://pubs.acs.org/doi/abs/10.1021/acs.jcim.9b00225>.
28. Daina A, Michielin O, Zoete V. SwissTargetPrediction: Updated data and new features for efficient prediction of protein targets of small molecules. *Nucleic Acids Res.* 2019;47(W1):W357–W364. <https://doi.org/10.1093/nar/gkz382>.
29. Szklarczyk D, Kirsch R, Koutrouli M, Nastou K, Mehryary F, Hachilif R, Gable AL, Fang T, Doncheva NT, Pyysalo S, Bork P, Jensen LJ, von Mering C. The STRING database in 2023: Protein-protein association networks and functional enrichment analyses for any sequenced genome of interest. *Nucleic Acids Res.* 2023;51(D1):D638–D646. <https://doi.org/10.1093/nar/gkac1000>.
30. Otasek D, Morris JH, Bouças J, Pico AR, Demchak B. Cytoscape automation: Empowering workflow-based network analysis. *Genome Biol.* 2019;20(1):185. <https://doi.org/10.1186/s13059-019-1758-4>.
31. Ge SX, Jung D, Yao R. ShinyGO: A graphical gene-set enrichment tool for animals and plants. *Bioinformatics.* 2020;36(8):2628–2629. <https://doi.org/10.1093/bioinformatics/btz931>.
32. Gao J, Aksoy BA, Dogrusoz U, Dresdner G, Gross B, Sumer SO, Sun Y, Jacobsen A, Sinha R, Larsson E, Cerami E, Sander C, Schultz N. Integrative analysis of complex cancer genomics and clinical profiles using the cBioPortal. *Sci Signal.* 2013;6(269):pl1. <https://doi.org/10.1126/scisignal.2004088>.
33. Ciriello G, Gatza ML, Beck AH, Wilkerson MD, Rhie SK, Pastore A, Zhang H, McLellan M, Yau C, Kandoth C, Bowlby R, Shen H, Hayat S, Fieldhouse

- R, Lester SC, Tse GM, Factor RE, Collins LC, Allison KH, Chen YY, Jensen K, Johnson NB, Oesterreich S, Mills GB, Cherniack AD, Robertson G, Benz C, Sander C, Laird PW, Hoadley KA, King TA; TCGA Research Network; Perou CM. Comprehensive molecular portraits of invasive lobular breast cancer. *Cell*. 2015;163(2):506–519. <https://doi.org/10.1016/j.cell.2015.09.033>.
34. Tang Z, Li C, Kang B, Gao G, Li C, Zhang Z. GEPIA: A web server for cancer and normal gene expression profiling and interactive analyses. *Nucleic Acids Res*. 2017;45(W1):W98–W102. <https://doi.org/10.1093/nar/gkx247>.
35. Li T, Fan J, Wang B, Traugh N, Chen Q, Liu JS, Li B, Liu XS. TIMER: A web server for comprehensive analysis of tumor-infiltrating immune cells. *Cancer Res*. 2017;77(21):e108–e110. <https://doi.org/10.1158/0008-5472.can-17-0307>.
36. Berman HM, Westbrook J, Feng Z, Gilliland G, Bhat TN, Weissig H, Shindyalov IN, Bourne PE. The Protein Data Bank. *Nucleic Acids Res*. 2000;28(1):235–242. <https://doi.org/10.1093/nar/28.1.235>.
37. Rowsell S, Hawtin P, Minshull CA, Jepson H, Brockbank SM, Barratt DG, Slater AM, McPheat WL, Waterson D, Henney AM, Pauitit RA. Crystal structure of human MMP-9 in complex with a reverse hydroxamate inhibitor. *J Mol Biol*. 2002;319(1):173–181. [https://doi.org/10.1016/s0022-2836\(02\)00262-0](https://doi.org/10.1016/s0022-2836(02)00262-0).
38. Wiederstein M, Sippl MJ. ProSA-web: Interactive web service for the recognition of errors in three-dimensional structures of proteins. *Nucleic Acids Res*. 2007;35(Web Server issue):W407–W410. <https://doi.org/10.1093/nar/gkm290>.
39. Dallakyan S, Olson AJ. Small-molecule library screening by docking with PyRx. *Methods Mol Biol*. 2015;1263:243–250. [https://doi.org/10.1007/978-1-4939-2269-7\\_19](https://doi.org/10.1007/978-1-4939-2269-7_19).
40. Lyu Y, Xiao Q, Yin L, Yang L, He W. Potent delivery of an MMP inhibitor to the tumor microenvironment with thermosensitive liposomes for the suppression of metastasis and angiogenesis. *Signal Transduct Target Ther*. 2019;4:26. <https://doi.org/10.1038/s41392-019-0054-9>.
41. Ozvoldik K, Stockner T, Krieger E. YASARA model-interactive molecular modeling from two dimensions to virtual realities. *J Chem Inf Model*. 2023;63(20):6177–6182. <https://doi.org/10.1021/acs.jcim.3c01136>.
42. Giordano D, Biancaniello C, Argenio MA, Facchiano A. Drug design by pharmacophore and virtual screening approach. *Pharmaceuticals (Basel)*. 2022;15(5):646. <https://doi.org/10.3390/ph15050646>.
43. Kar S, Leszczynski J. Exploration of computational approaches to predict the toxicity of chemical mixtures. *Toxics*. 2019;7(1):15. <https://doi.org/10.3390/toxics7010015>.
44. Raies AB, Bajic VB. In silico toxicology: Computational methods for the prediction of chemical toxicity. *Wiley Interdiscip Rev Comput Mol Sci*. 2016;6(2):147–172. <https://doi.org/10.1002/wcms.1240>.
45. Benchabane Y, Di Giorgio C, Boyer G, Sabatier AS, Allegro D, Peyrot V, De Méo M. Photo-inducible cytotoxic and clastogenic activities of 3,6-disubstituted acridines obtained by acylation of proflavine. *Eur J Med Chem*. 2009;44(6):2459–2467. <https://doi.org/10.1016/j.ejmech.2009.01.010>.
46. Lee Y, Choi SQ. Quantitative analysis for lipophilic drug transport through a model lipid membrane with membrane retention. *Eur J Pharm Sci*. 2019;134:176–184. <https://doi.org/10.1016/j.ejps.2019.04.020>.
47. Bennion BJ, Be NA, Mc Nerney MW, Lao V, Carlson EM, Valdez CA, Malfatti MA, Enright HA, Nguyen TH, Lightstone FC, Carpenter TS. Predicting a drug's membrane permeability: A computational model validated with in vitro permeability assay data. *J Phys Chem B*. 2017;121(20):5228–5237. <https://doi.org/10.1021/acs.jpbc.7b02914>.
48. Farkas JJ, Korcsmáros T, Kovács IA, Mihalik Á, Palotai R, Simkó GI, Szalay KZ, Szalay-Beko M, Vellai T, Wang S, Csermely P. Network-based tools for the identification of novel drug targets. *Sci Signal*. 2011;4(173):pt3. <https://doi.org/10.1126/scisignal.2001950>.
49. Hu G, Agarwal P. Human disease-drug network based on genomic expression profiles. *PLoS One*. 2009;4(8):e6536. <https://doi.org/10.1371/journal.pone.0006536>.
50. Pabon NA, Xia Y, Estabrooks SK, Ye Z, Herbrand AK, Süß E, Biondi RM, Assimon VA, Gestwicki JE, Brodsky JL, Camacho CJ, Bar-Joseph Z. Predicting protein targets for drug-like compounds using transcriptomics. *PLoS Comput Biol*. 2018;14(12):e1006651. <https://doi.org/10.1371/journal.pcbi.1006651>.
51. Augoff K, Hryniewicz-Jankowska A, Tabola R, Stach K. MMP9: A tough target for targeted therapy for cancer. *Cancers (Basel)*. 2022;14(7):1847. <https://doi.org/10.3390/cancers14071847>.
52. Sabit H, Arneht B, Abdel-Ghany S, Madyan EF, Ghaleb AH, Selvaraj P, Shin DM, Bommireddy R, Elhashash A. Beyond cancer cells: How the tumor microenvironment drives cancer progression. *Cells*. 2024;13(19):1666. <https://doi.org/10.3390/cells13191666>.
53. Mbeunkui F, Johann DJ Jr. Cancer and the tumor microenvironment: A review of an essential relationship. *Cancer Chemother Pharmacol*. 2009;63(4):571–582. <https://doi.org/10.1007/s00280-008-0881-9>.
54. Bijak V, Gucwa M, Lenkiewicz J, Murzyn K, Cooper DR, Minor W. Continuous validation across macromolecular structure determination process. *Nihon Kessho Gakkaishi*. 2023;65(1):10–16. <https://doi.org/10.5940/jcrsj.65.10>.
55. Chatterjee A, Walters R, Shafi Z, Ahmed OS, Sebek M, Gysi D, Yu R, Eliassi-Rad T, Barabási AL, Menichetti G. Improving the generalizability of protein-ligand binding predictions with AI-Bind. *Nat Commun*. 2023;14(1):1989. <https://doi.org/10.1038/s41467-023-37572-z>.
56. Seo S, Choi J, Park S, Ahn J. Binding affinity prediction for protein-ligand complex using deep attention mechanism based on intermolecular interactions. *BMC Bioinformatics*. 2021;22(1):542. <https://doi.org/10.1186/s12859-021-04466-0>.
57. Du X, Li Y, Xia YL, Ai SM, Liang J, Sang P, Ji XL, Liu SQ. Insights into protein-ligand interactions: Mechanisms, models, and methods. *Int J Mol Sci*. 2016;17(2):144. <https://doi.org/10.3390/ijms17020144>.
58. Lipinski CA. Rule of five in 2015 and beyond: Target and ligand structural limitations, ligand chemistry structure, and drug discovery project decisions. *Adv Drug Deliv Rev*. 2016;101:34–41. <https://doi.org/10.1016/j.addr.2016.04.029>.
59. Burton PS, Goodwin JT. Solubility and permeability measurement and applications in drug discovery. *Comb Chem High Throughput Screen*. 2010;13(2):101–111. <https://doi.org/10.2174/138620710790596763>.
60. Caldwell GW, Yan Z, Tang W, Dasgupta M, Hasting B. ADME optimization and toxicity assessment in early- and late-phase drug discovery. *Curr Top Med Chem*. 2009;9(11):965–980. <https://doi.org/10.2174/156802609789630929>.
61. Rauf A, Imran M, Khan IA, Ur-Rehman M, Gilani SA, Mehmood Z, Mubarak MS. Anticancer potential of quercetin: A comprehensive review. *Phytother Res*. 2018;32(11):2109–2130. <https://doi.org/10.1002/ptr.6155>.
62. Tao SF, He HF, Chen Q. Quercetin inhibits proliferation and invasion acts by up-regulating miR-146a in human breast cancer cells. *Mol Cell Biochem*. 2015;402(1–2):93–100. <https://doi.org/10.1007/s11010-014-2317-7>.
63. Atashpour S, Fouladdel S, Movahhed TK, Barzegar E, Ghahremani MH, Ostad SN, Azizi E. Quercetin induces cell cycle arrest and apoptosis in CD133(+) cancer stem cells of human colorectal HT29 cancer cell line and enhances anticancer effects of doxorubicin. *Iran J Basic Med Sci*. 2015;18(7):635–643.
64. Zhao J, Fang Z, Zha Z, Sun Q, Wang H, Sun M, Qiao B. Quercetin inhibits cell viability, migration and invasion by regulating miR-16/HOXA10 axis in oral cancer. *Eur J Pharmacol*. 2019;847:11–18. <https://doi.org/10.1016/j.ejphar.2019.01.006>.
65. Wang G, Wang Y, Yao L, Gu W, Zhao S, Shen Z, Lin Z, Liu W, Yan T. Pharmacological activity of quercetin: An updated review. *Evid Based Complement Alternat Med*. 2022;2022:3997190. <https://doi.org/10.1155/2022/3997190>.
66. Wu TC, Chan ST, Chang CN, Yu PS, Chuang CH, Yeh SL. Quercetin and chrysin inhibit nickel-induced invasion and migration by downregulation of TLR4/NF-κB signaling in A549 cells. *Chem Biol Interact*. 2018;292:101–109. <https://doi.org/10.1016/j.cbi.2018.07.010>.
67. Li H, Qiu Z, Li F, Wang C. The relationship between MMP-2 and MMP-9 expression levels with breast cancer incidence and prognosis. *Oncol Lett*. 2017;14(5):5865–5870. <https://doi.org/10.3892/ol.2017.6924>.
68. Kalali D. The role of the Matrix Metalloproteinase-9 gene in tumor development and metastasis: A narrative review. *Glob Med Genet*. 2023;10(2):48–53. <https://doi.org/10.1055/s-0043-1768166>.
69. Zeng Y, Gao M, Lin D, Du G, Cai Y. Prognostic and immunological roles of MMP-9 in pan-cancer. *Biomed Res Int*. 2022;2022:2592962. <https://doi.org/10.1155/2022/2592962>.

70. Mathpal S, Sharma P, Joshi T, Pande V, Mahmud S, Jeong MK, Obaidullah AJ, Chandra S, Kim B. Identification of zinc-binding inhibitors of matrix metalloproteinase-9 to prevent cancer through deep learning and molecular dynamics simulation approach. *Front Mol Biosci.* 2022;9:857430. <https://doi.org/10.3389/fmolb.2022.857430>.
71. Rashid ZA, Bardaweel SK. Novel matrix metalloproteinase-9 (MMP-9) inhibitors in cancer treatment. *Int J Mol Sci.* 2023;24(15):12133. <https://doi.org/10.3390/ijms241512133>.
72. Tandon A, Sinha S. Structural insights into the binding of MMP-9 inhibitors. *Bioinformation.* 2011;5(8):310–314.
73. Wulandari ET, Soetrisno, Purwanto B, Reviono, Ertanto Y, Sunowo J. A molecular docking insight: *Phyllanthus niruri* L. constituents targeting MMP-9 for angiogenesis inhibition and IL-1 $\beta$  for anti-inflammatory action in endometriosis therapy. *Plant Sci Today.* 2024;11(4):1–9. <https://doi.org/10.14719/pst.3224>.
74. Yosef G, Hayun H, Papo N. Simultaneous targeting of CD44 and MMP-9 catalytic and hemopexin domains as a therapeutic strategy. *Biochem J.* 2021;478(5):1139–1157. <https://doi.org/10.1042/bcj20200628>.
75. Underwood CK, Min D, Lyons JG, Hambley TW. The interaction of metal ions and Marimastat with matrix metalloproteinase-9. *J Inorg Biochem.* 2003;95(2):165–170. [https://doi.org/10.1016/s0162-0134\(03\)00100-4](https://doi.org/10.1016/s0162-0134(03)00100-4).
76. Ballav S, Lokhande KB, Dabhi I, Inje S, Ranjan A, Swamy KV, Basu S. Designing novel quercetin derivatives as matrix metalloproteinase-9 inhibitors in colon carcinoma: An in vitro and in silico approach. *J Dent Res Rev.* 2020;7(Suppl 1):S30. [https://doi.org/10.4103/jdr.jdrr\\_67\\_19](https://doi.org/10.4103/jdr.jdrr_67_19).
77. Saragusti AC, Ortega MG, Cabrera JL, Estrin DA, Marti MA, Chiabrande GA. Inhibitory effect of quercetin on matrix metalloproteinase-9 activity: Molecular mechanism and structure-activity relationship of the flavonoid-enzyme interaction. *Eur J Pharmacol.* 2010;644(1–3):138–145. <https://doi.org/10.1016/j.ejphar.2010.07.001>.
78. Jana S, Singh SK. Identification of selective MMP-9 inhibitors through multiple e-pharmacophore, ligand-based pharmacophore, molecular docking, and density functional theory approaches. *J Biomol Struct Dyn.* 2019;37(4):944–965. <https://doi.org/10.1080/07391102.2018.1444510>.
79. Messah ADV, Darmiati S, Rumende CM, Soemarwoto RA, Prihartono J, Asmarinah A, Fadilah F, Prawiningrum AF. Prediction of MMP-9 polymorphism impacts on MDR-TB by molecular simulation and network interaction. *Pharmacogn J.* 2022;14(6):833–841. <http://dx.doi.org/10.5530/pj.2022.14.176>.